Supporting Information for

A Linear Mass Concentration Detector for Solvent Gradient Polymer Separations

Emily H. Mordan,[1] James H. Wade,[2] Eric Pearce,[2] David M. Meunier,[2]* and Ryan C. Bailey[1]*

[1]*Department of Chemistry, University of Michigan, Ann Arbor, MI 48109 United States*

[2]*Core R&D Analytical Sciences, The Dow Chemical Company, Midland, MI 48667, Unites States*

TABLE OF CONTENTS

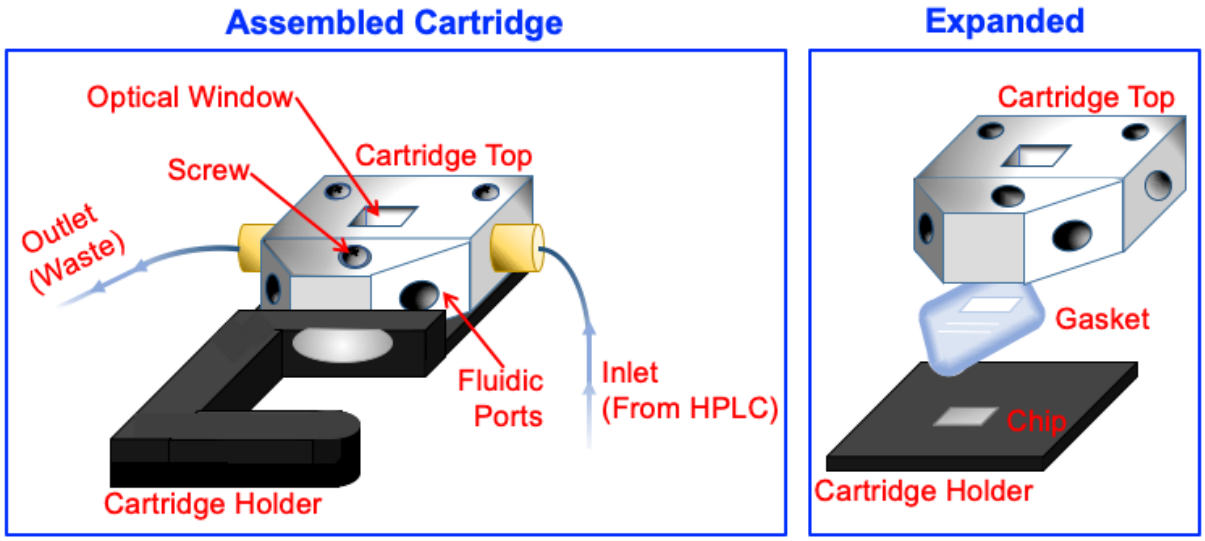

Figure S1: Microring Resonator Cartridge Assembly/HPLC Interface.
Sensor chip and gasket are sandwiched between cartridge top and holder, which is aligned and held in place by screws. The UV/visible detector is connected directly to one of the fluidic ports on the cartridge top, the gasket directs eluents across the rings, and waste exits the opposite port. Only one of two fluidic channels is used in this work.

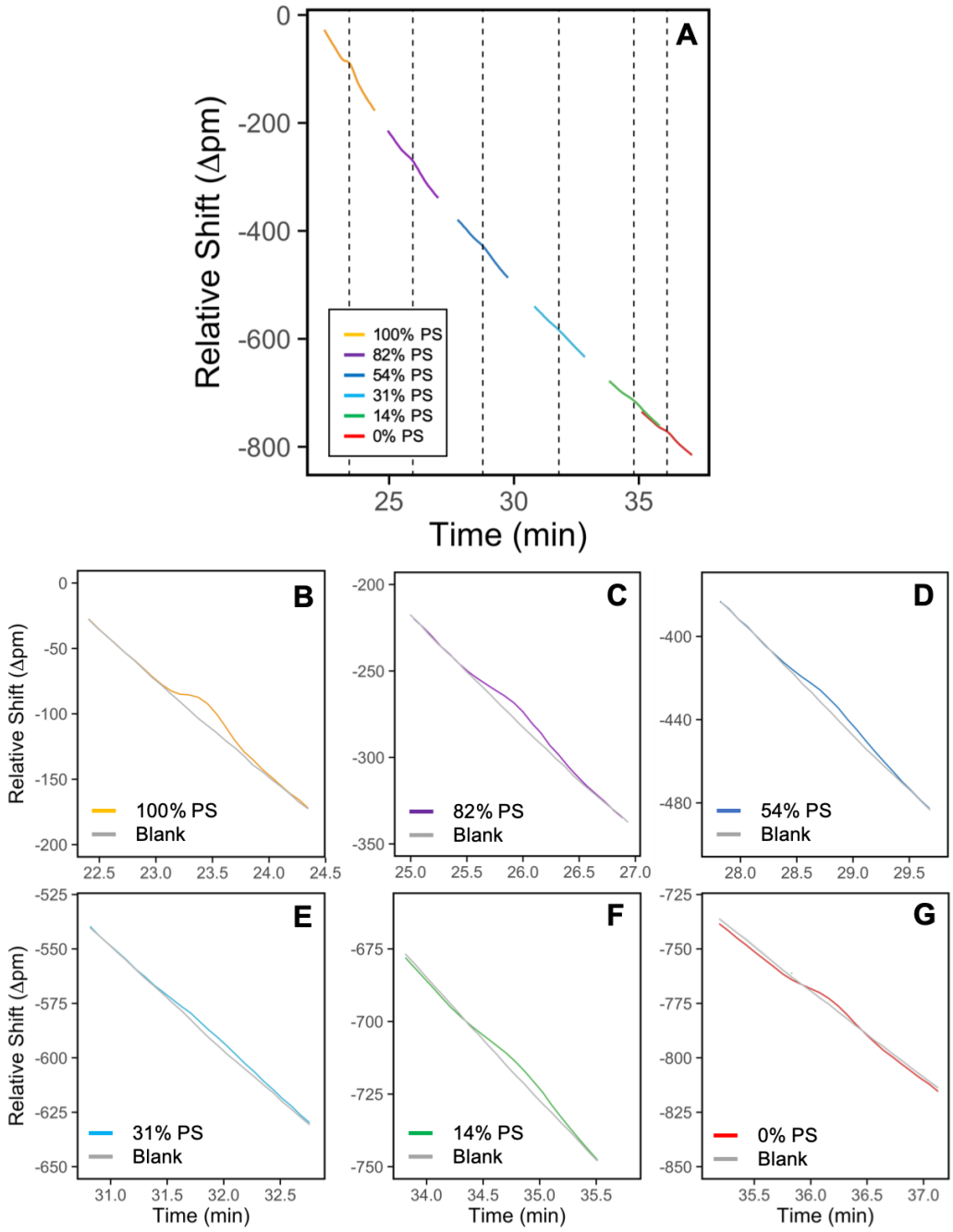

Figure S2: Closer Look at Peaks Before Baseline Correction.
A. The data from Figure 1B is plotted here highlighting only the portions of the traces that are relevant to peak location. The observed bumps or slight non-linearity on the slopping baseline coordinates to peak elution, which is not as visible in Figure 1B due to obstruction from overlapping baselines. Additionally, the dashed lines from Figure 1 are continued here to indicate peak location throughout the correction process. The relevant trace portions from **A** are plotted individually with a blank trace in panels **B-G**, allowing for the observation of peaks before baseline correction.

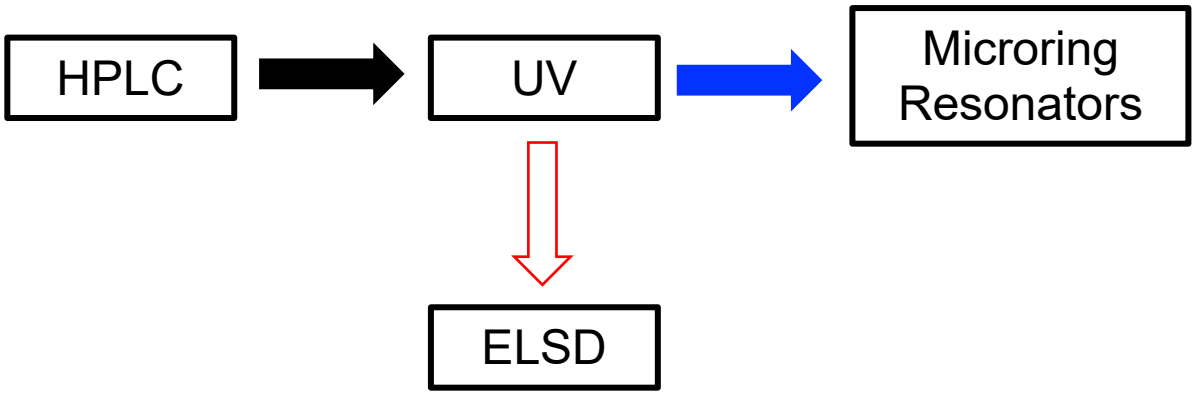

Figure S3: Fluidic Flow Path.
Eluents flow off the column to the UV detector and then the microring resonators which are connected in-line. The interface from figure S1 is represented here by the blue arrow. ELSD data needs to be collected last in series due to the destructive nature of the detector. ELSD data were collected in a separate experiment.

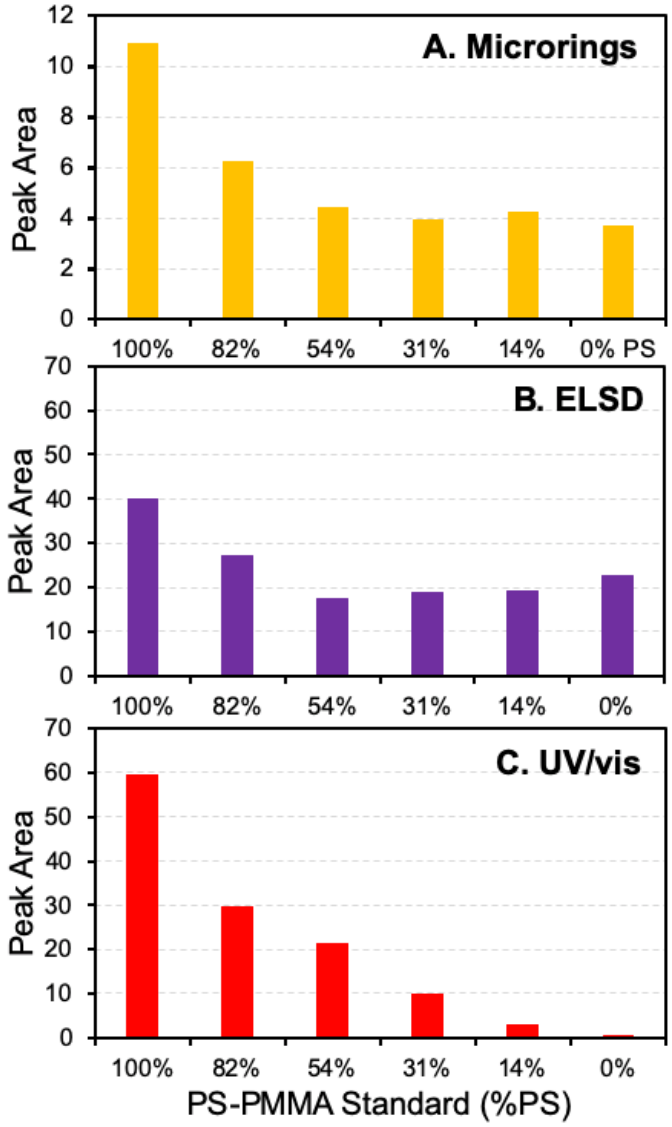

Figure S4: Peak Integrations for Gradient LC Chromatogram. Corresponding peak areas from Figure 2. **A.** Microring peak area decreases with decreasing RI contrast with increasing PMMA content. **B.** ELSD peak areas show a non-monotonic trend with polymer composition due to the solvent dependence and polymer composition dependence of the ELSD response. **C.** UV/vis peak areas decrease as a result of decreasing chromophore content/PS content.

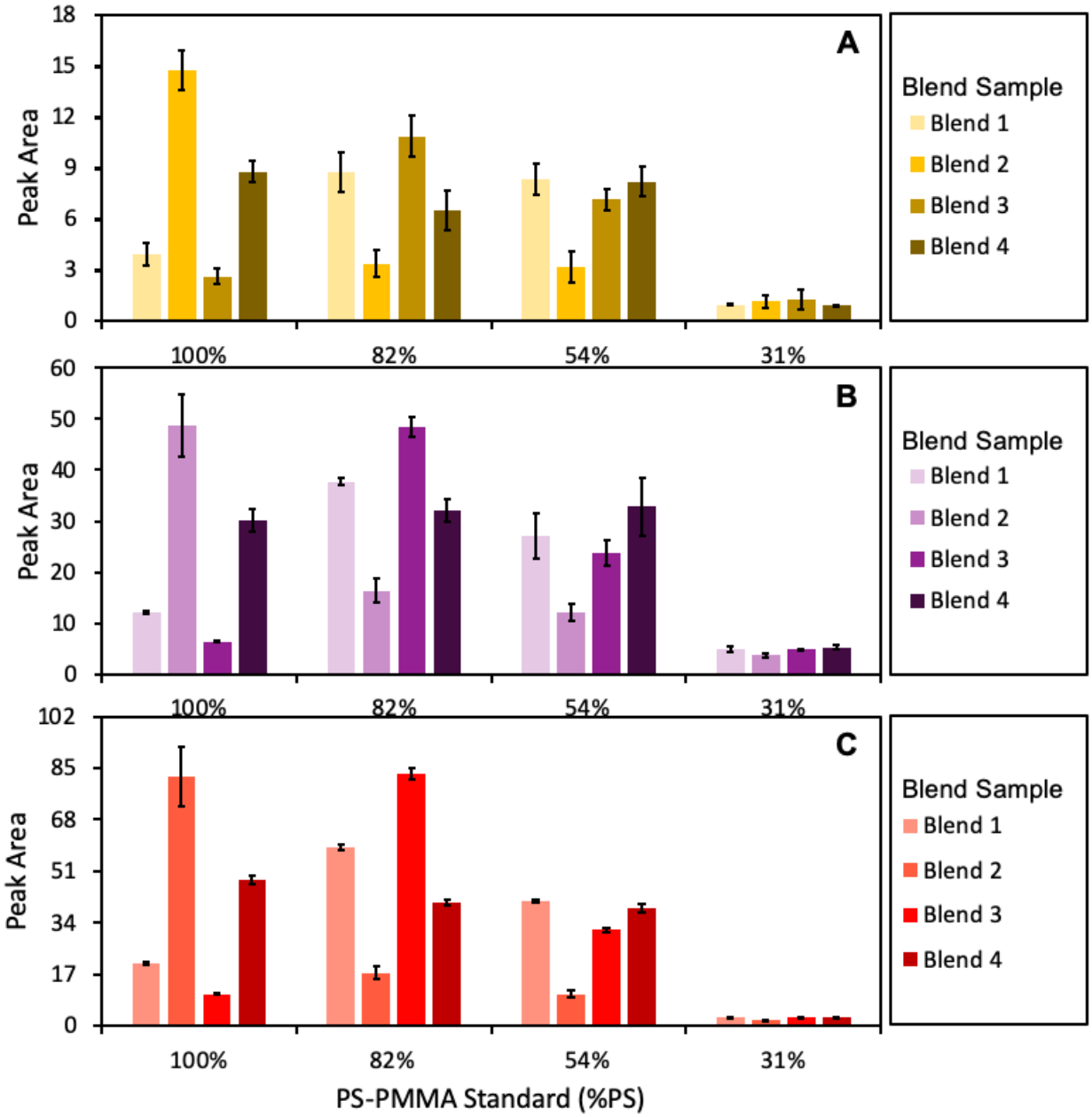

Figure S5: Peak Integrations for Polymer Blend Analysis.
Peak areas were integrated and then plugged into mass calibration curves to determine the mass of each blend component. Here is a comparison of these compiled peak areas, from the **A.** microring resonator, **B.** ELSD, and **C.** UV/vis.

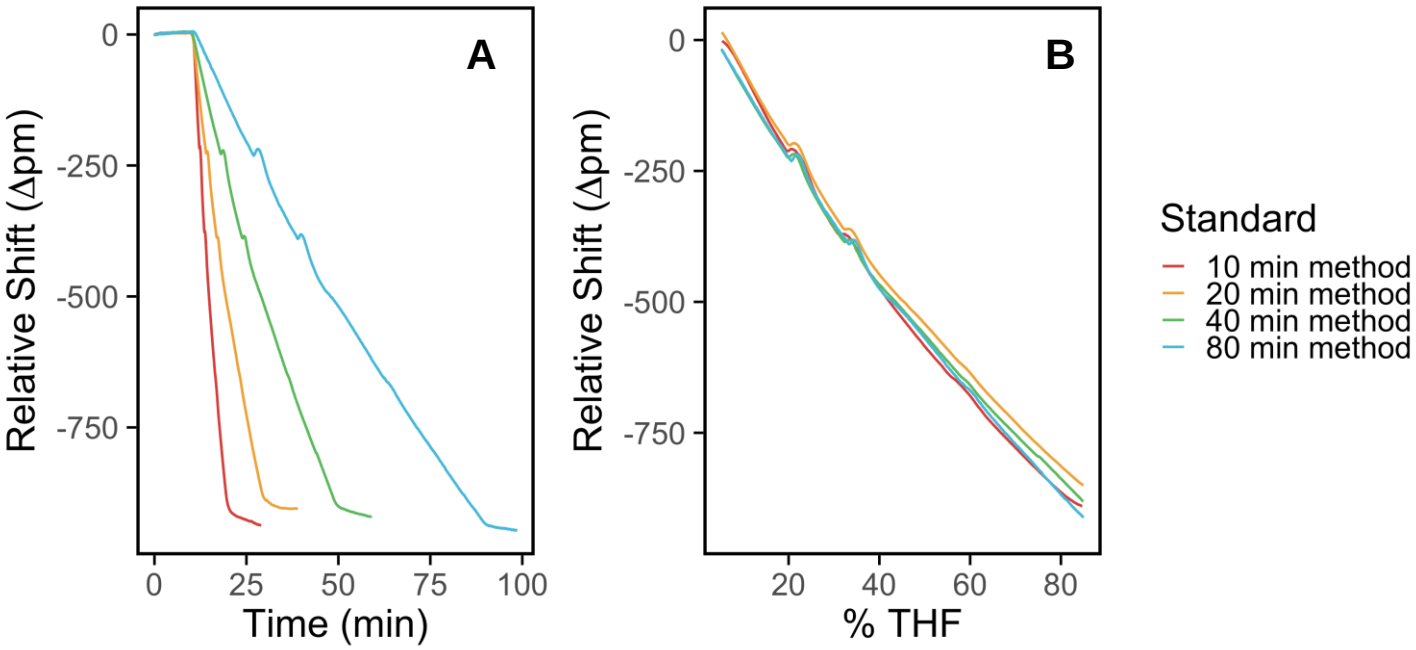

Figure S6: Investigation of Curvature in Raw Microring Traces. The slight curvature of the observed gradient traces suggests that the gradient may be too steep. **A.** However, upon investigation of gradient length the observed curvature was independent of time. **B.** The time independence was verified by plotting the traces as a function of nominal% THF. The time independence is likely due to the presence of 5% strong solvent (THF) in solvent A.

Table S1: Actual mass injected for each individual blend component

	Mass Injected for Each Blend Component (mg)				
	100% PS	82% PS-PMMA	54% PS-PMMA	31% PS-PMMA	Total Mass
Blend 1	0.09	0.28	0.33	0.05	0.75
Blend 2	0.52	0.09	0.09	0.05	0.75
Blend 3	0.05	0.42	0.24	0.05	0.75
Blend 4	0.23	0.19	0.28	0.05	0.75